

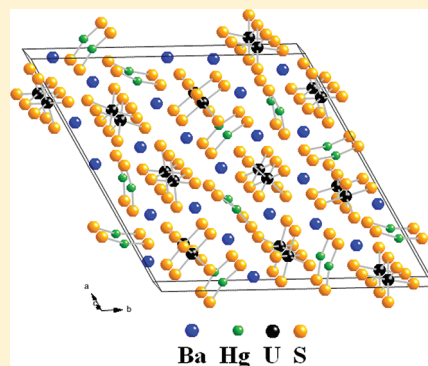
Ba₈Hg₃U₃S₁₈: A Complex Uranium(+4)/Uranium(+5) Sulfide

Daniel E. Bugaris and James A. Ibers*

Department of Chemistry, Northwestern University, 2145 Sheridan Road, Evanston, Illinois 60208-3113, United States

Supporting Information

ABSTRACT: The compound Ba₈Hg₃U₃S₁₈ was obtained from the solid-state reaction at 1123 K of U, HgS, BaS, and S, with BaBr₂/KBr or BaCl₂ as a flux. This material crystallizes in a new structure type in space group $P\bar{6}$ of the hexagonal system with three formula units in a cell of dimensions $a = 27.08(1)$ Å, $c = 4.208(2)$ Å, and $V = 2673(2)$ Å³. The structure contains infinite chains of US₆ octahedra and nearly linear [S–Hg–S]^{2–} dithiomercurate anions, separated by Ba²⁺ cations. In the temperature range 100–300 K, the paramagnetic behavior of Ba₈Hg₃U₃S₁₈ can be fit to the Curie–Weiss law, resulting in $\mu_{\text{eff}} = 5.40(4)$ μ_{B} , or 3.12(2) μ_{B}/U . The compound displays an antiferromagnetic transition at $T_{\text{N}} = 59$ K. Although the formal oxidation states of Ba, Hg, and S can be assigned as +2, +2, and –2, the oxidation state of U is less certain. On the basis of interatomic distance arguments and the magnetic susceptibility data, the compound is proposed to contain U in both +4 and +5 formal oxidation states.



INTRODUCTION

Ternary uranium chalcogenides (Q = chalcogen = S, Se, Te) have been extensively studied by the solid-state chemistry community.^{1,2} A number of these compounds exhibit interesting physical properties, including ferromagnetism in MnUSe₃,³ antiferromagnetism in M₂U₆Q_{15.5} (M = Rh, Ir; Q = S, Se),⁴ induced antiferromagnetism in MU₈Q₁₇ (M = Ti–Ni; Q = S, Se),⁵ and a transition from n-type to p-type semiconducting behavior in Cu_xUTe₃ ($x = 0.25$ and 0.33).⁶ The common link in all of these examples is that the formal oxidation state of U is +4. In chalcogenides, U can assume oxidation states ranging from +3 to +6, with tetravalent U being observed most often. For the interplay of theory and experiment, U⁵⁺ compounds offer the advantage of an f^1 configuration, as opposed to the f^2 configuration of U⁴⁺ compounds.⁷

However, there are only a limited number of known U⁵⁺ chalcogenides, including KUS₃,⁸ Rb₄U₄P₄Se₂₆,⁹ K₂Cu₃US₅,¹⁰ and Ti₃Cu₄USe₆.¹¹ The difficulty in synthesizing pentavalent uranium chalcogenides arises from the tendency of U⁵⁺ to disproportionate into U⁴⁺ and U⁶⁺ (UO₂²⁺) at the slightest hint of oxygen. However, less than total disproportionation of the U⁵⁺ species may result in the isolation of compounds with some mixture of the +4, +5, and +6 oxidation states. Several uranium oxides possessing some combination of these oxidation states have been reported.^{12–14} A few uranium chalcogenides with multiple oxidation states have also been reported, but these instead contain a mixture of U³⁺ and U⁴⁺ (trivalent uranium is stable in a chalcogenide environment but unknown for oxides).^{15–20} To the best of our knowledge, the only chalcogenide compound previously reported to contain both U⁴⁺ and U⁵⁺ is CsTiUTE₅,²¹ but the presence of Te–Te bonding complicates this assignment. We report here the synthesis, crystal structure, and magnetism of a rare example of a complex uranium sulfide that contains both U⁴⁺ and U⁵⁺.

EXPERIMENTAL METHODS

Syntheses. Uranium metal turnings (depleted, Oak Ridge National Laboratory) were converted to finely divided uranium powder by a modification²² of the literature procedure.²³ BaBr₂ (Alfa, 99.9%) and KBr (Mallinckrodt) in the molar ratio 48:52 were ground together with a mortar and pestle to produce the eutectic salt mixture with a melting point of 883 K.²⁴ The remaining reactants were used as obtained from the manufacturer. Reactions were performed in carbon-coated fused-silica tubes. The tubes were loaded with reaction mixtures under an argon atmosphere in a glovebox. The tubes were removed from the glovebox, evacuated to 10^{–4} Torr, and flame-sealed, before being placed in a computer-controlled furnace. Selected single crystals were examined by energy-dispersive X-ray (EDX) analyses on a Hitachi S-3400 scanning electron microscope.

Synthesis of Ba₈Hg₃U₃S₁₈. The reaction mixture consisted of U (0.13 mmol), HgS (0.19 mmol; Alfa Aesar), BaS (0.25 mmol; Alfa, 99.7%), S (0.31 mmol; Mallinckrodt, 99.6%), and a 48:52 molar ratio of BaBr₂/KBr (50 mg). The reaction mixture was placed in a furnace, where it was heated to 1173 K in 48 h, kept at 1173 K for 7 days, and cooled at 3 K h^{–1} to 673 K, and then the furnace was turned off. The product consisted of small black blocks of Ba₈Hg₃U₃S₁₈ in about 5 wt % yield (based on S), as well as red plates of BaHgS₂²⁵ and yellow plates of Ba₂HgS₃.²⁶ EDX analysis of selected crystals showed the presence of Ba, Hg, U, and S but not of K or Br. The compound was stable in air.

A crystal from this synthetic procedure was utilized for the collection of single-crystal X-ray diffraction data and subsequent structure determination. A synthesis with better reproducibility and higher yield was devised to yield sufficient material for the magnetic measurements. Here, the reaction mixture comprised a 8:3:3:7 stoichiometric combination of BaS, HgS, U, and S, along with BaCl₂ (200 mg) added as a flux. The heating profile was the same as that described above. The product consisted of a greater yield (~15 wt %) of black blocks of Ba₈Hg₃U₃S₁₈, as well as recrystallized HgS.

Received: October 5, 2011

Published: December 16, 2011

Structure Determination. Single-crystal X-ray diffraction data were collected with the use of graphite-monochromatized Mo $K\alpha$ radiation ($\lambda = 0.71073 \text{ \AA}$) at 215 K on a Bruker SMART 1000 CCD diffractometer.²⁷ The crystal-to-detector distance was 5.023 cm. Crystal decay was monitored by re-collecting 50 initial frames at the end of the data collection. Data were collected by a scan of 0.3° in ω in groups of 606 frames at φ settings of 0° , 90° , 180° , and 270° . The exposure time was 15 s frame^{-1} . The collection of intensity data was carried out with use of the program SMART.²⁷ Cell refinement and data reduction were carried out with use of the program SAINT v7.34a in APEX2.²⁸ Face-indexed absorption corrections were performed numerically with use of the program SADABS.²⁹ Then the program SADABS²⁹ was employed to make incident beam and decay corrections. The structure was solved with the direct-methods program SHELXS and refined with the least-squares program SHELXL.³⁰ The final refinement included anisotropic displacement parameters and a secondary extinction correction. The program STRUCTURE TIDY³¹ was used to standardize the positional parameters. Additional experimental details are given in Table 1 and in the Supporting Information. Selected metrical details are presented in Tables 2 and 3.

Table 1. Crystal Data and Structure Refinement for $\text{Ba}_8\text{Hg}_3\text{U}_3\text{S}_{18}$

formula	$\text{Ba}_8\text{Hg}_3\text{U}_3\text{S}_{18}$
fw	2991.66
space group	$P\bar{6}$
Z	3
a (\AA)	27.08(1)
c (\AA)	4.208(2)
V (\AA^3)	2673(2)
T (K)	215(2)
λ (\AA)	0.71073
ρ_c (g cm^{-3})	5.576
μ (mm^{-1})	36.175
$R(F)^a$	0.0274
$R_w(F^2)^b$	0.0590

^a $R(F) = \sum ||F_o| - |F_c|| / \sum |F_o|$ for $F_o^2 > 2\sigma(F_o^2)$. ^b $R_w(F_o^2) = \{ \sum [w(F_o^2 - F_c^2)^2] / \sum wF_o^4 \}^{1/2}$. For $F_o^2 < 0$, $w^{-1} = \sigma^2(F_o^2)$; for $F_o^2 \geq 0$, $w^{-1} = \sigma^2(F_o^2) + (0.0065F_o^2)^2$.

Table 2. Selected Interatomic Distances (\AA) for $\text{Ba}_8\text{Hg}_3\text{U}_3\text{S}_{18}$ ^a

Hg(1)–S(13)	2.344(4)	U(1)–S(4) \times 2	2.743(3)
Hg(1)–S(14)	2.345(4)	U(2)–S(5)	2.595(4)
Hg(2)–S(15)	2.345(4)	U(2)–S(6)	2.630(4)
Hg(2)–S(16)	2.352(4)	U(2)–S(7) \times 2	2.718(3)
Hg(3)–S(17)	2.348(4)	U(2)–S(8) \times 2	2.758(3)
Hg(3)–S(18)	2.351(4)	U(3)–S(9)	2.602(4)
U(1)–S(1)	2.571(4)	U(3)–S(10)	2.630(4)
U(1)–S(2)	2.615(4)	U(3)–S(11) \times 2	2.713(3)
U(1)–S(3) \times 2	2.729(3)	U(3)–S(12) \times 2	2.745(3)

^aAll atoms have crystallographic symmetry $m\cdots$

Table 3. Selected Interatomic Angles (deg) for $\text{Ba}_8\text{Hg}_3\text{U}_3\text{S}_{18}$

S(13)–Hg(1)–S(14)	164.0(1)	S(5)–U(2)–S(7)	92.1(1)
S(15)–Hg(2)–S(16)	165.2(1)	S(5)–U(2)–S(8)	88.0(1)
S(17)–Hg(3)–S(18)	166.2(1)	S(7)–U(2)–S(7)	101.5(1)
S(1)–U(1)–S(2)	179.0(1)	S(7)–U(2)–S(8)	179.0(1)
S(1)–U(1)–S(4)	90.8(1)	S(9)–U(3)–S(10)	176.2(1)
S(1)–U(1)–S(3)	89.5(1)	S(9)–U(3)–S(11)	92.0(1)
S(3)–U(1)–S(3)	100.9(1)	S(9)–U(3)–S(12)	88.7(1)
S(3)–U(1)–S(4)	179.6(1)	S(11)–U(3)–S(11)	101.7(1)
S(5)–U(2)–S(6)	176.1(1)	S(11)–U(3)–S(12)	178.9(1)

Magnetic Susceptibility Measurement. Magnetic susceptibility as a function of the temperature was measured on a 4.87 mg sample of ground single crystals of $\text{Ba}_8\text{Hg}_3\text{U}_3\text{S}_{18}$ with the use of a Quantum Design MPMS5 SQUID magnetometer. The sample was loaded into a gelatin capsule. Both zero-field-cooled (ZFC) and field-cooled (FC) susceptibility data were collected between 2 and 300 K at an applied field of 500 G. All data were corrected for electron core diamagnetism,³² as well as for the diamagnetism of the sample container.

RESULTS AND DISCUSSION

Syntheses. Black single crystals of $\text{Ba}_8\text{Hg}_3\text{U}_3\text{S}_{18}$ were obtained in 5 wt % yield by the reaction of U, HgS, BaS, S, and a BaBr_2/KBr eutectic salt mixture at 1173 K. The BaBr_2/KBr eutectic salt mixture has a lower melting point (883 K) than either of the individual salts (1120 and 1003 K, respectively) and is crucial for crystallization of the final product. The alternative synthetic procedure involves a stoichiometric combination of the reactants but uses BaCl_2 instead of the BaBr_2/KBr eutectic salt mixture. In this case, BaCl_2 (mp = 1198 K) may not be molten at the reaction temperature and may serve only as a nucleation site rather than a reaction medium. This is compensated for by the increased amounts of BaS and S in the reaction mixture. Efforts to synthesize the selenide and telluride analogues by either route were unsuccessful as only crystals of binary mercury and uranium chalcogenides, along with amorphous material, were obtained.

Structure. $\text{Ba}_8\text{Hg}_3\text{U}_3\text{S}_{18}$ crystallizes in a new structure type (Figure 1) in space group $P\bar{6}$ of the hexagonal system. The asymmetric unit of $\text{Ba}_8\text{Hg}_3\text{U}_3\text{S}_{18}$ contains eight Ba atoms, three Hg atoms, three U atoms, and 18 S atoms, for a total of 32 crystallographically unique atoms, all with site symmetry $m\cdots$. Each U atom is octahedrally coordinated by six S atoms. The three Hg atoms are each coordinated to two S atoms in a nearly linear geometry. Of the eight Ba atoms, Ba(2) and Ba(7) are each coordinated by seven S atoms in a monocapped trigonal prism of S atoms; the remaining Ba atoms are each coordinated to eight S atoms in a bicapped trigonal-prismatic arrangement.

The structure of $\text{Ba}_8\text{Hg}_3\text{U}_3\text{S}_{18}$ has some unusual features. Each US_6 octahedron shares edges with neighboring US_6 octahedra in the [001] direction to form infinite ${}^1[\text{US}_4]$ chains (Figure 2). Compounds containing uranium chalcogenide chains are extremely rare, with a few examples being CsUTe_6 ,²¹ $\text{Cs}_8\text{Hf}_3\text{UTe}_{30.6}$,²¹ and $\text{Ba}_4\text{Cr}_2\text{US}_9$.³³ Much more common are two-dimensional-layered uranium chalcogenide compounds.¹ To the best of our knowledge, this is the first example of a ternary or quaternary uranium chalcogenide to contain isolated chains of UQ_6 octahedra that do not share vertices, edges, or faces with neighboring transition-metal or uranium chalcogenide moieties. For example, CsCuUSe_3 ³⁴ has infinite ${}^1[\text{USe}_4]$ chains in the [100] direction, but each USe_6 octahedron in those chains also shares four edges with neighboring CuSe_4 tetrahedra. $\text{Ba}_8\text{Hg}_3\text{U}_3\text{S}_{18}$ may also be compared to BaUS_3 .³⁵ This compound has no transition metal, but because it adopts the perovskite structure, each US_6 octahedron shares all six vertices with neighboring octahedra to form a three-dimensional framework rather than isolated chains.

Another interesting structural feature in $\text{Ba}_8\text{Hg}_3\text{U}_3\text{S}_{18}$ is the presence of discrete, nearly linear $[\text{S}–\text{Hg}–\text{S}]^{2-}$ dithiomercurate anions. Two-coordinate linear Hg is commonly found in chalcogenides; however, it is nearly always contained within chains ($\text{K}_2\text{Hg}_3\text{S}_4$),³⁶ layers ($\text{Na}_2\text{Hg}_3\text{S}_4$),³⁷ or frameworks ($\text{K}_2\text{Hg}_6\text{S}_7$).³⁸ The only known examples of compounds to contain discrete dithiomercurate anions are A_2HgS_2 ($\text{A} = \text{Na}, \text{K}$)³⁹ and BaHgS_2 .²⁵ The isoelectronic $[\text{O}–\text{Hg}–\text{O}]^{2-}$ dioxomercurate anion

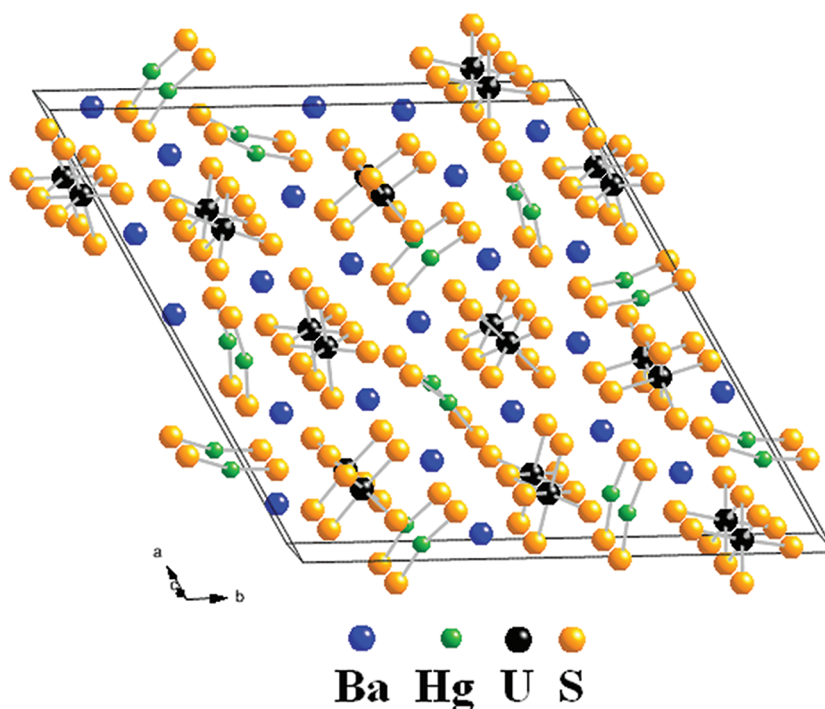


Figure 1. View down [001] of the crystal structure of $\text{Ba}_8\text{Hg}_3\text{U}_3\text{S}_{18}$.

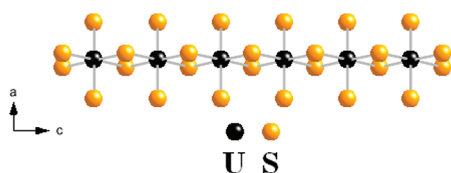


Figure 2. Infinite one-dimensional ${}^1[\text{US}_4]$ chains in $\text{Ba}_8\text{Hg}_3\text{U}_3\text{S}_{18}$ as viewed down [010].

is similarly rare, found only in compounds A_2HgO_2 ($\text{A} = \text{Li}-\text{Cs}$),⁴⁰ SrHgO_2 ,⁴¹ and BaHgO_2 .⁴² Related $[\text{P}-\text{Hg}-\text{P}]^{4-}$ and $[\text{As}-\text{Hg}-\text{As}]^{4-}$ linear anions are found in A_4HgP_2 ($\text{A} = \text{Na}, \text{K}$)⁴³ and K_4HgAs_2 ,⁴⁴ respectively.

Magnetic Susceptibility. The magnetic susceptibility of $\text{Ba}_8\text{Hg}_3\text{U}_3\text{S}_{18}$ for both ZFC and FC data, as a function of the temperature, is shown in Figure 3. The magnetic susceptibility exhibits a maximum at $T_N = 59$ K, indicative of an antiferromagnetic transition. There are numerous examples of ternary and quaternary uranium sulfides that exhibit antiferromagnetic transitions, including MU_8S_{17} ($\text{M} = \text{V}-\text{Ni}$),⁵ RhUS_3 ,⁴⁵ and $\text{Ir}_2\text{U}_6\text{S}_{15.5}$.⁴ The Néel temperatures range from a low of 19 K in VU_8S_{17} to a high of 61 K in $\text{MnU}_8\text{S}_{17}$. $\text{K}_2\text{Cu}_3\text{US}_5$ ¹⁰ has the appearance of an antiferromagnetic transition at 104 K, but this has been attributed to a possible magnetic or structural phase change coupled to a $\text{Cu}-\text{U}$ charge transfer.

For $\text{Ba}_8\text{Hg}_3\text{U}_3\text{S}_{18}$, the inverse magnetic susceptibility data (Figure 4) vary linearly with temperature above 100 K and can be fit to the Curie–Weiss law $\chi^{-1} = (T - \theta_p)/C$. The values of the Curie constant C and the Weiss constant θ_p are $3.65(5)$ emu K mol^{-1} and $-60(3)$ K, respectively. The effective magnetic moment, μ_{eff} as calculated from the equation $\mu_{\text{eff}} = (7.997C)^{1/2} \mu_B$,⁴⁶ is $5.40(4) \mu_B$.

Formal Oxidation States. Because there are no S–S bonds in $\text{Ba}_8\text{Hg}_3\text{U}_3\text{S}_{18}$, each S can be considered as a S^{2-} anion. Ba is +2 as an alkaline-earth cation, and the Ba··S distances of $3.123(3)-3.556(4)$ Å in $\text{Ba}_8\text{Hg}_3\text{U}_3\text{S}_{18}$ are comparable to those

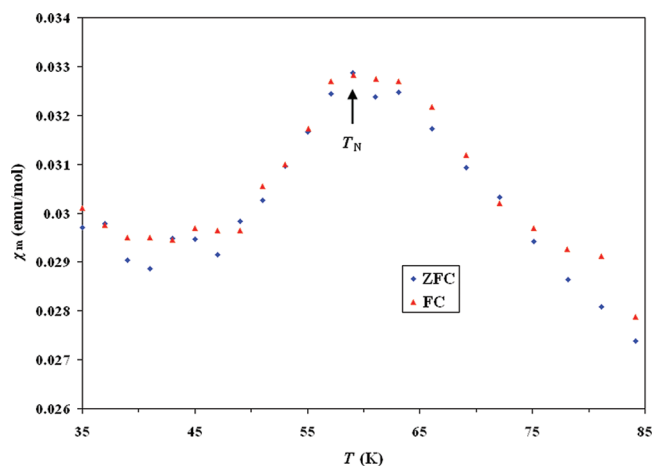


Figure 3. Magnetic susceptibility (χ_m) versus T for $\text{Ba}_8\text{Hg}_3\text{U}_3\text{S}_{18}$. The maximum is $T_N = 59$ K.

of $3.093(4)-3.510(5)$ Å found in $\text{Ba}_4\text{Cr}_2\text{US}_9$.³³ The Hg–S interatomic distances of $2.344(4)-2.352(4)$ Å in $\text{Ba}_8\text{Hg}_3\text{U}_3\text{S}_{18}$ are consistent with those of $2.31(1)-2.36(1)$ Å in BaHgS_2 ,²⁵ which contains the linear dithiomercurate anion. Because the mercurous cation (Hg_2^{2+}) is highly unstable and readily disproportionates to Hg^{2+} and $\text{Hg}_{(\text{liq})}$, the present compound must contain Hg^{2+} in the form of approximately linear HgS_2 units.

Therefore, the combined formal oxidation states of the three U atoms in $\text{Ba}_8\text{Hg}_3\text{U}_3\text{S}_{18}$ must be +14 to maintain charge neutrality. This can be achieved either by the presence of multiple formal oxidation states for U [i.e., (i) U^{3+} , U^{5+} , and U^{6+} ; (ii) U^{4+} , U^{4+} , and U^{6+} ; or (iii) U^{4+} , U^{5+} , and U^{5+}] in the compound or by U in an intermediate (nonintegral) oxidation state.

A number of solid-state U compounds have been proposed to contain U in more than one formal oxidation state. Some examples of oxides include $\text{Cs}_2\text{K}(\text{UO}_2)_2\text{Si}_4\text{O}_{12}$ ¹² with both U^{4+}

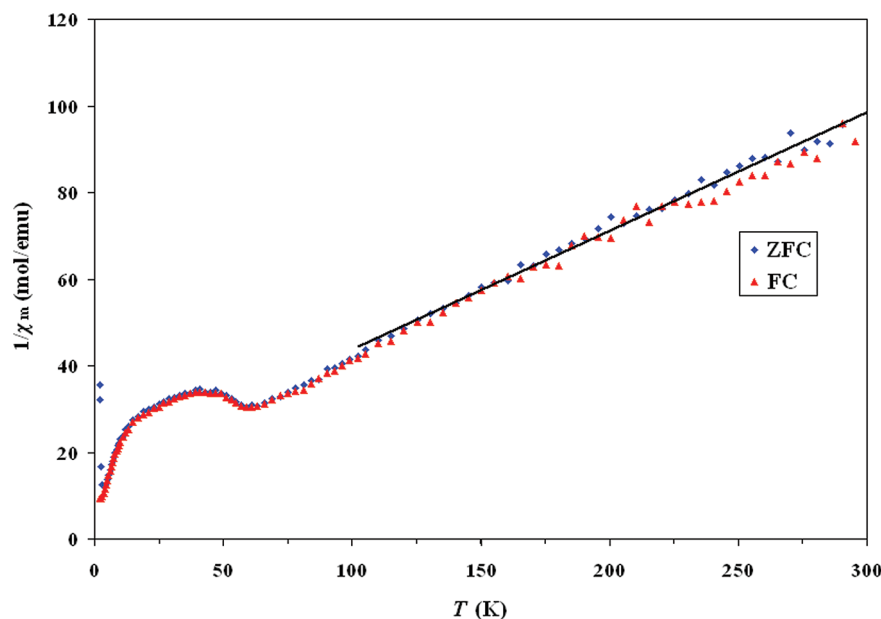


Figure 4. Inverse magnetic susceptibility ($1/\chi_m$) versus T for $\text{Ba}_8\text{Hg}_3\text{U}_3\text{S}_{18}$ showing a straight-line Curie–Weiss fit to the data.

and U^{5+} , $\text{Cs}_8\text{U}(\text{UO}_2)_3(\text{Ge}_3\text{O}_9)_3 \cdot 3\text{H}_2\text{O}^{13}$ with both U^{4+} and U^{6+} , and $\text{A}_3(\text{U}_2\text{O}_4)(\text{Ge}_2\text{O}_7)$ ($\text{A} = \text{Rb}, \text{Cs}$)¹⁴ with both U^{5+} and U^{6+} . The assignment of the oxidation states of U is more straightforward in oxides than it is in chalcogenides for two reasons. First, there are no reported examples of simple U^{3+} oxides, which reduces the number of possible oxidation states by one. Second, in oxides U^{6+} is almost always present as the uranyl ion, UO_2^{2+} , so that U has two significantly shorter $\text{U}=\text{O}$ axial bonds (~ 1.8 Å) that are not present for U^{4+} or U^{5+} . Few exceptions to this rule exist, with one notable example being $\delta\text{-UO}_3$,^{47,48} which has a regular octahedron of O atoms surrounding U^{6+} . For $\text{Cs}_2\text{K}(\text{UO}_2)\text{Si}_4\text{O}_{12}$, there is one crystallographic U site, with the shortest U–O interatomic distance being 2.1232(2) Å, which is too long for uranyl bonds. Therefore, for charge balance, the U site must contain a 1:1 ratio of U^{4+} and U^{5+} . $\text{Cs}_8\text{U}(\text{UO}_2)_3(\text{Ge}_3\text{O}_9)_3 \cdot 3\text{H}_2\text{O}$ has two distinct U sites, one of which has a tetragonal-bipyramidal coordination with short axial U–O bonds (1.812 Å) indicative of the presence of U^{6+} . The charge balance and regular octahedral coordination of the other site suggest an oxidation state of +4 for U. In the $\text{A}_3(\text{U}_2\text{O}_4)(\text{Ge}_2\text{O}_7)$ ($\text{A} = \text{Rb}, \text{Cs}$) compounds, there are three different crystallographic U sites. Two of the sites have short U–O bond lengths (≤ 1.840 Å) consistent with U^{6+} , whereas the shortest U–O interatomic distance at the third site is 1.991 Å, which implies U^{5+} for charge balance. It should be noted that for these oxide compounds the formal oxidation state assignments were supported by some combination of X-ray photoelectron spectroscopy, X-ray absorption near-edge structure, and magnetic susceptibility measurements.

The assignment of mixed or multiple oxidation states in chalcogenides is more challenging owing to the possible presence of U^{3+} , the lack of a characteristic bonding structure for U^{6+} , and the potential for Q–Q bonding (which means that not all Q anions can simply be considered as Q^{2-} units). One of the simpler cases involves the U_3Q_5 ($\text{Q} = \text{S}, \text{Se}$) compounds^{15,16} which possess two crystallographically distinct U sites: a seven-coordinate site containing U^{3+} , and an eight-coordinate site containing U^{4+} . Because there is no Q–Q bonding, this allows the compound to be formulated as $(\text{U}^{3+})_2(\text{U}^{4+})(\text{Q}^{2-})_5$, which charge balances. This

formal oxidation state assignment for U has been supported by magnetic susceptibility data, as well as by analogy to the rare-earth derivatives, i.e., Ln_2UQ_5 or $(\text{Ln}^{3+})_2(\text{U}^{4+})(\text{Q}^{2-})_5$.⁴⁹ In U_3Te_5 ,¹⁷ which is not isostructural with the sulfide and selenide analogues, there are three crystallographically distinct U sites, each in a bicapped trigonal-prismatic environment of Te anions. The U–Te interatomic lengths for one site are noticeably shorter than those for the other two U sites, suggesting a higher valence (U^{4+}) for this site versus the other two sites with U^{3+} . Some uranium chalcogenides have been theorized to contain U in an intermediate (nonintegral) oxidation state. For example, in uranium monochalcogenides, a $5f^{3-\delta}$ electronic configuration for U was postulated on the basis of magnetic and optical measurements.⁵⁰ Because it is not clear how sensitive such measurements are as indicators of the electronic configuration of U, we favor the simpler interpretation of mixed oxidation states in such compounds, such as those described above for $\text{Cs}_2\text{K}(\text{UO}_2)\text{Si}_4\text{O}_{12}$.¹² Some combination of both U^{3+} and U^{4+} on the same crystallographic site is expected for each of the following three compounds that possess a single U site with U–Q interatomic distances intermediate between those expected for U^{3+} and U^{4+} : $\text{Cu}_2\text{U}_3\text{S}_7$,¹⁸ Mo_6US_8 ,¹⁹ and $\text{Pd}_3\text{U}_{0.92}\text{S}_4$.²⁰ For the compound CsTiUTe_5 ,²¹ some combination of U^{4+} and U^{5+} is to be expected on the single U crystallographic site. If this compound only contained Te^{2-} anions, charge balance would dictate an oxidation state of +5 for U. However, the presence of short Te–Te interactions complicates the oxidation state assignment and increases the likelihood of having both U^{4+} and U^{5+} in this compound.

Returning now to $\text{Ba}_8\text{Hg}_3\text{U}_3\text{S}_{18}$, we need to consider the possible combinations of formal oxidation states that would require that the total charge on the three crystallographically independent U sites be +14, namely, (i) U^{3+} , U^{5+} , and U^{6+} ; (ii) U^{4+} , U^{4+} , and U^{6+} ; or (iii) U^{4+} , U^{5+} , and U^{5+} . The most common oxidation state for U in chalcogenide compounds is +4. Although more often observed with halides, U^{3+} is known for a select few chalcogenides, including UTe_2 ,⁵¹ U_3Q_5 ($\text{Q} = \text{S}, \text{Se}$),^{15,16} U_2Q_3 ($\text{Q} = \text{S}, \text{Se}, \text{Te}$),^{52–54} ScUS_3 ,⁵⁵ and ScU_3S_6 .⁵⁶ The only reported U^{5+} chalcogenides in the literature are KUS_3 ,⁸ $\text{Rb}_4\text{U}_4\text{P}_4\text{Se}_{26}$,⁹ $\text{K}_2\text{Cu}_3\text{US}_5$,¹⁰ and $\text{Tl}_3\text{Cu}_4\text{USe}_6$.¹¹ The single example of a U^{6+}

Table 4. Comparison of the Average U–S Interatomic Distances for Compounds Containing US_6 Octahedra

compound	U–S range (Å)	average U–S interatomic distance (Å) ^a	U oxidation state
$K_6Cu_{12}U_2S_{15}$ ^b	2.615(6)	2.615	+5 or +6
$K_2Cu_3US_5$ ^c	2.587(1)–2.6827(9)	2.651	+5
$Ba_8Hg_3U_3S_{18}$	U(1)	2.571(4)–2.743(3)	+4 and +5
	U(2)	2.595(4)–2.758(3)	+4 and +5
	U(3)	2.602(4)–2.745(3)	+4 and +5
$KCuUS_3$ ^d	2.714(1)–2.7165(9)	2.715	+4
$RbCuUS_3$ ^d	2.7085(8)–2.718(1)	2.715	+4
$CsCuUS_3$ ^d	2.7064(7)–2.7232(9)	2.718	+4
$Ba_2Cu_2US_5$ ^e	2.673(2)–2.770(1)	2.738	+4
$RbAgUS_3$ ^d	2.747(2)–2.759(2)	2.751	+4
$CsAgUS_3$ ^d	2.750(1)–2.759(1)	2.753	+4

^aNo estimated standard deviation is given because the individual U–S distances differ significantly. ^bReference 57. ^cReference 10. ^dReference 67. ^eReference 70.

chalcogenide is $A_6Cu_{12}U_2S_{15}$ ($A = K, Rb, Cs$),^{57,58} although this has also been postulated as a U^{5+} compound by invoking mixed S^{2-}/S^- oxidation states (as seen for other copper sulfides, such as $K_2Cu_2CeS_4$ ⁵⁹ and CuS ⁶⁰).

The U–S interatomic distances in $Ba_8Hg_3U_3S_{18}$ can provide some insight about the oxidation state of U. The average U–S interatomic distances for U(1), U(2), and U(3) in $Ba_8Hg_3U_3S_{18}$, as well as for other compounds with US_6 octahedra, are given in Table 4. We have found no compounds in the literature with U^{3+} octahedrally coordinated by S^{2-} anions, but because the ionic radius of U^{3+} is larger than that of U^{4+} (1.025 vs 0.89 Å),⁶¹ we expect that the U^{3+} –S interatomic distances would be about 0.13 Å longer than a U^{4+} –S distance. Clearly, the average U–S interatomic distances in $Ba_8Hg_3U_3S_{18}$ are shorter than those in the compounds containing U^{4+} but longer than the U–S interatomic distances for U^{5+} or U^{6+} compounds. This favors combination (iii); namely, both U^{4+} and U^{5+} are present in $Ba_8Hg_3U_3S_{18}$.

The values of the free-ion moments for U, as calculated from LS coupling, are $3.62 \mu_B$ (U^{3+}), $3.58 \mu_B$ (U^{4+}), and $2.54 \mu_B$ (U^{5+}).⁶² Because it possesses no f electrons, U^{6+} is diamagnetic. For the formal oxidation state assignments listed above, the calculated effective magnetic moments for $Ba_8Hg_3U_3S_{18}$ are $4.42 \mu_B$ (i), $5.06 \mu_B$ (ii), and $5.07 \mu_B$ (iii). The measured effective magnetic moment for $Ba_8Hg_3U_3S_{18}$ is $5.40(4) \mu_B$, which is significantly larger than the calculated value for (i) and closer to the calculated values for (ii) or (iii). From the measured magnetic susceptibility, a value of $\mu_{\text{eff}} = 3.12(2) \mu_B/U$ can be determined, which falls between the theoretical values for U^{4+} and U^{5+} , and could be another indicator of mixed valency on the U site. However, this value is also consistent with the effective magnetic moments measured for U^{4+} chalcogenides, including MU_8Q_{17} ($M = Ti-Ni$; $Q = S, Se$; $3.0-3.6 \mu_B/U$),⁵ $Ir_2U_6S_{15.5}$ ($3.26 \mu_B/U$),⁴ and $Tl_{1.12}U_2Te_6$ ($3.27 \mu_B/U$).⁶³ Magnetic measurements are not sufficiently sensitive to distinguish oxidation states for U.

Bond valence sum analysis⁶⁴ provides an empirical method of assigning formal oxidation states. The BondValence Function in *PLATON*⁶⁵ provides the following valencies for $Ba_8Hg_3U_3S_{18}$: U(1) 4.20; U(2) 4.10; U(3) 4.14; Hg(1) 1.98; Hg(2) 1.97; Hg(3) 1.96; Ba(1) 2.15; Ba(2) 2.17; Ba(3) 2.18; Ba(4) 2.16; Ba(5) 2.17; Ba(6) 2.13; Ba(7) 2.30; Ba(8) 2.22. These empirical calculations imply a +4 oxidation state for U, but their accuracy for uranium chalcogenides is uncertain. Consider the $AMUQ_3$ ($A = K, Rb, Cs$; $M = Cu, Ag, Au$; $Q = S, Se, Te$)^{21,34,66-68} series of compounds as an example. In this family, a formal oxidation state of +4 for U has been confirmed by

thorough structural analysis (analogous to Zr^{4+} and Hf^{4+} phases) and charge-balance considerations. However, bond valence sum analysis of the sulfide members⁶⁹ reveals bond valence sums for U ranging from 3.42 to 3.84. Therefore, in the current example of $Ba_8Hg_3U_3S_{18}$, the bond valence sums for U of 4.10 to 4.20 may, in fact, be consistent with a higher valence than 4, i.e., a mixture of U^{4+} and U^{5+} , again combination (iii).

CONCLUSION

A complex uranium sulfide, $Ba_8Hg_3U_3S_{18}$, has been synthesized by a reactive flux technique, and its structure has been determined by single-crystal X-ray diffraction methods. Simple charge-balance considerations fail to identify the formal oxidation state of U in this compound. Thus, we have utilized interatomic distances and bond valence sum calculations, magnetic susceptibility measurements, and analogy to other mixed-oxidation-state U compounds to infer that in the structure of $Ba_8Hg_3U_3S_{18}$ there are one U^{4+} cation and two U^{5+} cations randomly distributed over the three U crystallographic sites. Hence, $Ba_8Hg_3U_3S_{18}$ appears to be a rare example of a solid-state uranium chalcogenide that contains U^{5+} , an oxidation state that is especially interesting because of its f^1 configuration. Ongoing research will attempt to determine the synthetic conditions that favor the formation of pentavalent uranium in chalcogenides and related compounds.

ASSOCIATED CONTENT

Supporting Information

X-ray crystallographic file in CIF format for $Ba_8Hg_3U_3S_{18}$. This material is available free of charge via the Internet at <http://pubs.acs.org>.

AUTHOR INFORMATION

Corresponding Author

*E-mail: ibers@chem.northwestern.edu.

ACKNOWLEDGMENTS

Funding for this research was kindly provided by the U.S. Department of Energy, Basic Energy Sciences, Chemical Sciences, Biosciences, and Geosciences Division and Division of Materials Science and Engineering (Grant ER-15522). Magnetic measurements were made at the Materials Research Science and Engineering Center, Magnet and Low Temperature Facility, supported by the National Science Foundation (Grant DMR05-20513).

REFERENCES

- (1) Narducci, A. A.; Ibers, J. A. *Chem. Mater.* **1998**, *10*, 2811–2823.
- (2) Grenthe, I.; Drozdowski, J.; Fujino, T.; Buck, E. C.; Albrecht-Schmitt, T. E.; Wolf, S. F. In *The Chemistry of the Actinide and Transactinide Elements*, 3rd ed.; Morss, L. R., Edelstein, N. M., Fuger, J., Eds.; Springer: Dordrecht, The Netherlands, 2006; Vol. 1, pp 253–698.
- (3) Ijjaali, I.; Mitchell, K.; Huang, F. Q.; Ibers, J. A. *J. Solid State Chem.* **2004**, *177*, 257–261.
- (4) Daoudi, A.; Noël, H. *J. Alloys Compd.* **1996**, *233*, 169–173.
- (5) Noel, H.; Troc, R. *J. Solid State Chem.* **1979**, *27*, 123–135.
- (6) Patschke, R.; Breshers, J. D.; Brazis, P.; Kannewurf, C. R.; Billinge, S. J. L.; Kanatzidis, M. G. *J. Am. Chem. Soc.* **2001**, *123*, 4755–4762.
- (7) Graves, C. R.; Kiplinger, J. L. *Chem. Commun.* **2009**, *45*, 3831–3853.
- (8) Padiou, J.; Guillevic, J. C. R. *Seances Acad. Sci., Ser. C* **1969**, *268*, 822–824.
- (9) Chondroudis, K.; Kanatzidis, M. G. *J. Am. Chem. Soc.* **1997**, *119*, 2574–2575.
- (10) Gray, D. L.; Backus, L. A.; Krug von Nidda, H.-A.; Skanthakumar, S.; Loidl, A.; Soderholm, L.; Ibers, J. A. *Inorg. Chem.* **2007**, *46*, 6992–6996.
- (11) Bugaris, D. E.; Choi, E. S.; Copping, R.; Glans, P.-A.; Minasian, S. G.; Tyliczak, T.; Kozimor, S. A.; Shuh, D. K.; Ibers, J. A. *Inorg. Chem.* **2011**, *50*, 6656–6666.
- (12) Lee, C.-S.; Wang, S.-L.; Lii, K.-H. *J. Am. Chem. Soc.* **2009**, *131*, 15116–15117.
- (13) Nguyen, Q. B.; Liu, H.-K.; Chang, W.-J.; Lii, K.-H. *Inorg. Chem.* **2011**, *50*, 4241–4243.
- (14) Lin, C.-H.; Lii, K.-H. *Angew. Chem., Int. Ed.* **2008**, *47*, 8711–8713.
- (15) Moseley, P. T.; Brown, D.; Whittaker, B. *Acta Crystallogr.* **1972**, *B28*, 1816–1821.
- (16) Noël, H.; Prigent, J. *Physica B + C* **1980**, *102*, 372–379.
- (17) Tougait, O.; Potel, M.; Noël, H. *J. Solid State Chem.* **1998**, *139*, 356–361.
- (18) Daoudi, A.; Lamire, M.; Levet, J. C.; Noël, H. *J. Solid State Chem.* **1996**, *123*, 331–336.
- (19) Daoudi, A.; Potel, M.; Noël, H. *J. Alloys Compd.* **1996**, *232*, 180–185.
- (20) Daoudi, A.; Noël, H. *Inorg. Chim. Acta* **1986**, *117*, 183–185.
- (21) Cody, J. A.; Ibers, J. A. *Inorg. Chem.* **1995**, *34*, 3165–3172.
- (22) Bugaris, D. E.; Ibers, J. A. *J. Solid State Chem.* **2008**, *181*, 3189–3193.
- (23) Haneveld, A. J. K.; Jellinek, F. *J. Less-Common Met.* **1969**, *18*, 123–129.
- (24) Roth, R. S.; Negas, T.; Cook, L. P. *Phase Diagrams for Ceramists*; American Ceramic Society: Columbus, OH, 1983; Vol. V; p 5, Figure 5600.
- (25) Rad, H. D.; Hoppe, R. Z. *Anorg. Allg. Chem.* **1981**, *483*, 18–25.
- (26) Rad, H. R.; Hoppe, R. Z. *Anorg. Allg. Chem.* **1981**, *483*, 7–17.
- (27) SMART Version 5.054 Data Collection and SAINT-Plus Version 6.45a Data Processing Software for the SMART System; Bruker Analytical X-ray Instruments, Inc.: Madison, WI, 2003.
- (28) APEX2 Version 2009.5-1 and SAINT Version 7.34a Data Collection and Processing Software; Bruker Analytical X-ray Instruments, Inc.: Madison, WI, 2009.
- (29) Sheldrick, G. M. SADABS; Department of Structural Chemistry, University of Göttingen: Göttingen, Germany, 2008.
- (30) Sheldrick, G. M. *Acta Crystallogr. Sect. A: Found. Crystallogr.* **2008**, *64*, 112–122.
- (31) Gelato, L. M.; Parthé, E. *J. Appl. Crystallogr.* **1987**, *20*, 139–143.
- (32) Mulay, L. N.; Boudreaux, E. A., Eds. *Theory and Applications of Molecular Diamagnetism*; Wiley-Interscience: New York, 1976.
- (33) Yao, J.; Ibers, J. A. *Z. Anorg. Allg. Chem.* **2008**, *634*, 1645–1647.
- (34) Huang, F. Q.; Mitchell, K.; Ibers, J. A. *Inorg. Chem.* **2001**, *40*, 5123–5126.
- (35) Brochu, R.; Padiou, J.; Grandjean, D. *C. R. Seances Acad. Sci., Ser. C* **1970**, *271*, 642–643.
- (36) Kanatzidis, M. G.; Park, Y. *Chem. Mater.* **1990**, *2*, 99–101.
- (37) Klepp, K. O. *J. Alloys Compd.* **1992**, *182*, 281–288.
- (38) Axtell, E. A. III; Park, Y.; Chondroudis, K.; Kanatzidis, M. G. *J. Am. Chem. Soc.* **1998**, *120*, 124–136.
- (39) Klepp, K. O.; Prager, K. Z. *Naturforsch., B: Anorg. Chem., Org. Chem.* **1992**, *47*, 491–496.
- (40) Hoppe, R.; Roehrborn, H.-J. *Naturwissenschaften* **1962**, *49*, 419–420.
- (41) Soll, M.; Müller-Buschbaum, H. *J. Less-Common Met.* **1991**, *175*, 295–299.
- (42) Soll, M.; Müller-Buschbaum, H. *J. Less-Common Met.* **1990**, *162*, 169–174.
- (43) Eisenmann, B.; Somer, M. Z. *Naturforsch., B: J. Chem. Sci.* **1989**, *44*, 1228–1232.
- (44) Asbrand, M.; Eisenmann, B.; Somer, M. Z. *Kristallogr.—New Cryst. Struct.* **1997**, *212*, 79.
- (45) Daoudi, A.; Noël, H. *Inorg. Chim. Acta* **1987**, *140*, 93–95.
- (46) O'Connor, C. J. *Prog. Inorg. Chem.* **1982**, *29*, 203–283.
- (47) Wait, E. *J. Inorg. Nucl. Chem.* **1955**, *1*, 309–312.
- (48) Weller, M. T.; Dickens, P. G.; Penny, D. J. *Polyhedron* **1988**, *7*, 243–244.
- (49) Tien, V.; Guittard, M.; Flahaut, J.; Rodier, N. *Mater. Res. Bull.* **1975**, *10*, 547–554.
- (50) Noël, H. *J. Solid State Chem.* **1984**, *52*, 203–210.
- (51) Beck, H. P.; Dausch, W. Z. *Naturforsch., B: J. Chem. Sci.* **1988**, *43*, 1547–1550.
- (52) Zachariasen, W. H. *Acta Crystallogr.* **1949**, *2*, 291–296.
- (53) Khodadad, P. C. R. *Hebd. Seances Acad. Sci.* **1959**, *249*, 694–696.
- (54) Tougait, O.; Potel, M.; Levet, J. C.; Noël, H. *Eur. J. Solid State Inorg. Chem.* **1998**, *35*, 67–76.
- (55) Julien, R.; Rodier, N.; Tien, V. *Acta Crystallogr., Sect. B: Struct. Crystallogr. Cryst. Chem.* **1978**, *34*, 2612–2614.
- (56) Rodier, N.; Tien, V. *Acta Crystallogr., Sect. B: Struct. Crystallogr. Cryst. Chem.* **1976**, *32*, 2705–2707.
- (57) Sutorik, A. C.; Patschke, R.; Schindler, J.; Kannewurf, C. R.; Kanatzidis, M. G. *Chem.—Eur. J.* **2000**, *6*, 1601–1607.
- (58) Yao, J.; Jin, G. B.; Malliakas, C.; Wells, D. M.; Ellis, D. E.; Kanatzidis, M. G.; Ibers, J. A., unpublished results.
- (59) Sutorik, A. C.; Albritton-Thomas, J.; Kannewurf, C. R.; Kanatzidis, M. G. *J. Am. Chem. Soc.* **1994**, *116*, 7706–7713.
- (60) Folmer, J. C. W.; Jellinek, F. *J. Less-Common Met.* **1980**, *76*, 153–162.
- (61) Shannon, R. D. *Acta Crystallogr., Sect. A: Cryst. Phys., Diffr., Theor. Gen. Crystallogr.* **1976**, *32*, 751–767.
- (62) Kittel, C. *Introduction to Solid State Physics*, 7th ed.; Wiley: New York, 1996.
- (63) Tougait, O.; Daoudi, A.; Potel, M.; Noël, H. *Mater. Res. Bull.* **1997**, *32*, 1239–1245.
- (64) Brown, I. D. *The Chemical Bond in Inorganic Chemistry, The Bond Valence Model*; Oxford University Press: New York, 2002.
- (65) Spek, A. L. *PLATON, A Multipurpose Crystallographic Tool*; Utrecht University: Utrecht, The Netherlands, 2008.
- (66) Sutorik, A. C.; Albritton-Thomas, J.; Hogan, T.; Kannewurf, C. R.; Kanatzidis, M. G. *Chem. Mater.* **1996**, *8*, 751–761.
- (67) Yao, J.; Wells, D. M.; Chan, G. H.; Zeng, H.-Y.; Ellis, D. E.; Van Duyn, R. P.; Ibers, J. A. *Inorg. Chem.* **2008**, *47*, 6873–6879.
- (68) Bugaris, D. E.; Ibers, J. A. *J. Solid State Chem.* **2009**, *182*, 2587–2590.
- (69) Wells, D. M.; Jin, G. B.; Skanthakumar, S.; Haire, R. G.; Soderholm, L.; Ibers, J. A. *Inorg. Chem.* **2009**, *48*, 11513–11517.
- (70) Zeng, H.-yi; Yao, J.; Ibers, J. A. *J. Solid State Chem.* **2008**, *181*, 552–555.